Proceedings of the 2017 18th
International Conference on Advanced Robotics (ICAR)
Hong Kong, China, July 2017

A Practical Calibration Method for Spinal Surgery Robot

Yinghao Ning
Shenzhen Graduate School, Harbin Institute of Technology
Shenzhen Institutes of Advanced Technology, Chinese Academy of Sciences
Shenzhen, Guangdong Province, China
ty_nyh@sina.com

Peng Gao
Shenzhen Institutes of Advanced Technology, Chinese Academy of Sciences
Shenzhen, Guangdong Province, China
peng.gao@siat.ac.cn

Yu Sun
Shenzhen Institutes of Advanced Technology, Chinese Academy of Sciences
Shenzhen, Guangdong Province, China
yu.sun@siat.ac.cn

Xiaozhi Qi*
Shenzhen Institutes of Advanced Technology, Chinese Academy of Sciences
Shenzhen, Guangdong Province, China
xz.qi@siat.ac.cn

Ying Hu*
Shenzhen Institutes of Advanced Technology, Chinese Academy of Sciences
Shenzhen, Guangdong Province, China
ying.hu@siat.ac.cn

***Abstract* - Surgery robot for pedicle screw placement is explored based on parallel manipulator. To improve the accuracy of parallel manipulator, a practical calibration algorithm is mainly discussed. At the beginning, a novel measurement scheme for calibration is proposed. In order to construct the error model, the propagation of error is analyzed and the procedures for constructing error model are particularly developed. A new algorithm for identifications of parameters is proposed based on particle swarm method. Finally, experiment for calibration is conducted to verify the effectiveness of calibration algorithm. Experiment of pedicle screw placement with spine of pig is carried out to confirm the precision of manipulator after calibration.**

***Index Terms* - Pedicle screw placement, parallel manipulator, kinematic calibration.**

I. INTRODUCTION

Medical surgery robots are receiving tremendous attention in surgeries due to its advantageous performance such as theirs high accuracy and stability. One of examples using medical surgery robots used to support and improve the stability of the surgery, is pedicle screw placement. Fig. 1 depicts the surgery of pedicle screw placement. High precision are required in this operation because of the possible damage to the nerves and blood vessels. With the help of surgery robots, it is capable to avoid some risks of the surgery produced by surgeons, such as that from hand tremor and tiredness.

Surgery robots, developed during these years, can be classified into two basic configurations: series robot [1][2], due to its huge workspace, and parallel robot [3][4], because of its perfect stiffness. In the surgery of pedicle screw placement, parallel manipulator has greater potential than series manipulator, with overall consideration of the workspace and stiffness. In this article, a robotic surgery system is being developed based on parallel manipulator.

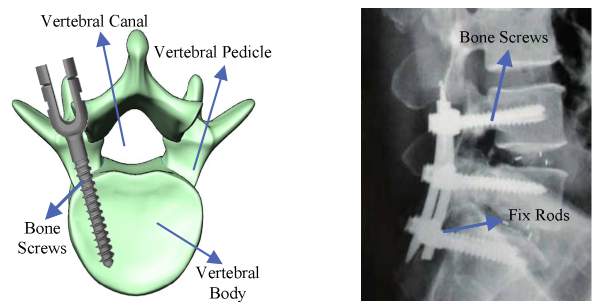

(a) Structure of the vertebrae (b) Scheme of the operation
Fig. 1 The pedicle screw placement

As the fact that, for parallel manipulator, position and orientation of end effector are crucial factors in the medical surgery of pedicle screw placement, the process of kinematic calibration is indispensable to improve the precision of robots. A practical calibration process is a supplement, besides the quality of design, manufacture and assembly, for improving the precision before manipulators are used in the surgeries. Usually kinematic calibration can be classified into two categories: self-calibration [5] and outer calibration [6], and outer calibration is used for calibration in this article due to its convenience of measurement equipment. Kinematic calibration consists of four steps: construction of error model, measurement of translation and orientation of mobile platform, kinematic parameter identification, and kinematic parameter compensation. The four steps can be carried out for several times in series to reduce the error to desired value.

The error model can be obtained through two ways: numerical method [7] and analytical method [6]. The numerical method can be obtained concisely without considering the complicated calculation of equation. Besides, the result from numerical method is the same as that of analytical method and anyone of the two methods is effective. Therefore, numerical method for the construction of error model is carried out preferentially.

* Corresponding authors.

978-1-5386-3157-7/17/$31.00 ©2017 IEEE

Kinematic parameter identification is a process of multi-objective optimization. Usually least square method is used to identify the error of kinematic parameter [7]. However, least square method cannot be effective enough, for some of kinematic parameters are tightly coupled, which make values of these parameters after identification are extremely high. The reason for such situation is that parameters cannot be confined to a particular range. Several intelligent optimization algorithms are well developed nowadays and they already show great potential in multi-objective optimization for kinematic parameter identification [8].

This article focuses on calibration method for spinal surgery robot. Firstly, robotic system for pedicle screw placement is discussed based on parallel manipulator. Then the scheme of measurement for the translation and orientation of mobile platform is proposed. The propagation of error is particularly discussed, not only for kinematic parameters but assembly errors of fixture. The algorithm with particle swarm optimization is explored for the kinematic parameters identification. Last experiments are conducted to verify the theory.

II. Measurement Scheme for Calibration

The robotic system for pedicle screw placement can be concisely viewed in Fig. 2. The system consists of human body, operation table, support frame and surgical robot. Fig. 2(b) depicts the overall structure for the surgical robot, which includes Stewart parallel manipulator, reflective marker spheres and guiding tube.

A. Kinematic Parameters

The factor causing error of translation and orientation for mobile platform usually can be grouped into two categories: factors that can be calibrated such as parameters of spherical joint, prismatic joint, as shown in Fig. 3, and so on; factors that cannot be calibrated such as tolerance in joints, random error and so on. Here just factors that can be calibrated are considered when building the error model.

Fig. 3 shows the prototype of parallel manipulator, Stewart Parallel manipulator, which includes base platform, mobile platform and six kinematic chains. Every chain consists of two spherical joints and one prismatic joint. For a spherical joint, there are 3 parameters depicting the position of spherical joint in the base coordinate system and 1 parameter for the prismatic joint. Therefore 7 kinematic parameters must be needed considering a kinematic chain and 42 kinematic parameters for the total parallel manipulator. These kinematic parameters will be identified in the identification procedure. There is an actuation for prismatic joint of every chain.

$$\Delta \boldsymbol{Y} = \boldsymbol{J}\Delta \boldsymbol{X} \tag{1}$$

where, $\Delta \boldsymbol{Y}$ is the error matrix of translation and orientation for mobile platform; $\boldsymbol{J}$ is the Jacobi matrix constructed with the error model; $\Delta \boldsymbol{X}$ is the matrix for error of kinematic parameters. The goal for construction of error model is to obtain Jacobin matrix $\boldsymbol{J}$, while the process of measurement with Laser Tracker is $\Delta \boldsymbol{Y}$. The operation to get $\Delta \boldsymbol{X}$ in formula (1) is so called parameter identification.

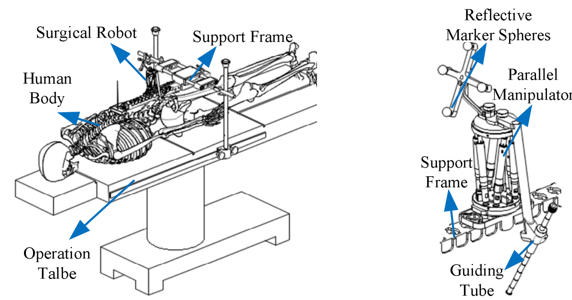

(a) The system for pedicle screw placement (b) Surgical robot

Fig. 2 Robotic system for pedicle screw placement

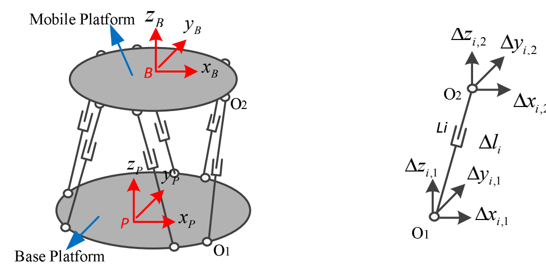

(a) Parallel manipulator (b) The ***i*** th chain

Fig. 3 Prototype of parallel manipulator

For the parallel manipulator, with the consideration of kinematic parameters only, $\Delta \boldsymbol{X}$ is the 42×1 matrix due to the number of kinematic parameters is 42. The row number of $\boldsymbol{J}$ matrix is related to the group number of measurement. If the group number for measurement is n, $\boldsymbol{J}$ is $(6\times n)\times 42$ matrix. $\Delta \boldsymbol{Y}$ is $(6\times n)\times 1$ matrix. If assembly errors α, β, λ, n_1, n_2, n_3 of fixture mounted onto the mobile platform, discussed later, are considered, $\Delta \boldsymbol{X}$ is the 48×1 matrix and $\boldsymbol{J}$ is $(6\times n)\times 48$ matrix, while $\Delta \boldsymbol{Y}$ is $(6\times n)\times 1$ matrix.

B. Measurement Scheme

In Fig. 4, there are three black target holders in the fixture to define ***A*** coordinate system in the fixture. In Fig. 5, coordinate system of ***O*** is global coordinate system defined by Laser Tracker. The ***A*** coordinate system is defined by fixture installing target ball of Laser Tracker and the ***A'*** coordinate system is one after movement. The ***B*** coordinate system is attached to the mobile platform of parallel manipulator and ***B'*** coordinate system is the one after the movement of mobile platform.

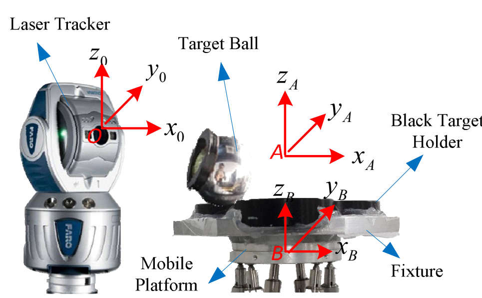

Fig.4 Measurement scheme

In the measurement scheme, the goal is to obtain the position and orientation of ***B'*** coordinate system with respect to ***B*** coordinate system. The symbol ${}^{B}_{B'}\boldsymbol{R}$ represents the orientation of $\boldsymbol{B'}$ coordinate system with respect to coordinate system of $\boldsymbol{B}$, and can be derived by the equations (2) to (5)

$$ {}^{B}_{B'}\boldsymbol{R} = ({}^{O}_{B}\boldsymbol{R})^{-1}\,{}^{o}_{B'}\boldsymbol{R} \tag{2} $$

where,

$$ {}^{O}_{B}\boldsymbol{R} = {}^{O}_{A}\boldsymbol{R}\,{}^{A}_{B}\boldsymbol{R} \tag{3} $$

$$ {}^{O}_{B'}\boldsymbol{R} = {}^{O}_{A'}\boldsymbol{R}\,{}^{A'}_{B'}\boldsymbol{R} \tag{4} $$

therefore,

$$ \begin{aligned} {}^{B}_{B'}\boldsymbol{R} &= ({}^{O}_{B}\boldsymbol{R})^{-1}\,{}^{o}_{B'}\boldsymbol{R} \\ &= ({}^{O}_{A}\boldsymbol{R}\,{}^{A}_{B}\boldsymbol{R})^{-1}({}^{O}_{A'}\boldsymbol{R}\,{}^{A'}_{B'}\boldsymbol{R}) \\ &= {}^{A}_{B}\boldsymbol{R}^{-1}\,{}^{O}_{A}\boldsymbol{R}^{-1}\,{}^{o}_{A'}\boldsymbol{R}\,{}^{A'}_{B'}\boldsymbol{R} \end{aligned} \tag{5} $$

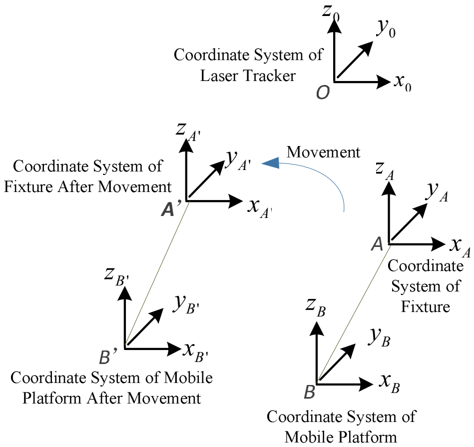

Fig. 5 Coordinate systems in measurement scheme

Meanings for symbols from the equations (2) to (5) can be defined as follows. For example, the symbol ${}^{O}_{B}\boldsymbol{R}$ represents the transformation matrix of $\boldsymbol{B}$ coordinate system in terms of $\boldsymbol{O}$ coordinate system. ${}^{O}_{B}\boldsymbol{R}$ is unit orthogonal matrix, which means columns (or rows) in ${}^{O}_{B}\boldsymbol{R}$ are unit vectors and orthogonal to one another.

Except for the orientation, the position of $\boldsymbol{B'}$ coordinate system with respect to $\boldsymbol{B}$ coordinate system is another data needed to be known after measurement. It can be written as follows

$$ {}^{B}\boldsymbol{P}_{BB'} = {}^{B}_{O}\boldsymbol{R}\,{}^{O}\boldsymbol{P}_{BB'} \tag{6} $$

${}^{O}\boldsymbol{P}_{BB'}$ is the $\boldsymbol{BB'}$ vector with respect to $\boldsymbol{O}$ coordinate system and can be derived by equations (7)-(9)

$$ {}^{O}\boldsymbol{P}_{BB'} = {}^{O}\boldsymbol{P}_{OB'} - {}^{O}\boldsymbol{P}_{OB} \tag{7} $$

where,

$$ {}^{O}\boldsymbol{P}_{OB} = {}^{O}\boldsymbol{P}_{OA} + {}^{O}\boldsymbol{P}_{AB} \tag{8} $$

$$ {}^{O}\boldsymbol{P}_{OB'} = {}^{O}\boldsymbol{P}_{OA'} + {}^{O}\boldsymbol{P}_{A'B'} \tag{9} $$

Therefore, ${}^{B}\boldsymbol{P}_{BB'}$ can be written as follows

$$ \begin{aligned} {}^{B}\boldsymbol{P}_{BB'} &= {}^{B}_{O}\boldsymbol{R}\,{}^{O}\boldsymbol{P}_{BB'} \\ &= ({}^{O}_{A}\boldsymbol{R}\,{}^{A}_{B}\boldsymbol{R})^{-1}({}^{O}\boldsymbol{P}_{OA'} + {}^{O}\boldsymbol{P}_{A'B'} - {}^{O}\boldsymbol{P}_{OA} - {}^{O}\boldsymbol{P}_{AB}) \\ &= {}^{A}_{B}\boldsymbol{R}^{-1}\,{}^{O}_{A}\boldsymbol{R}^{-1}\,{}^{O}\boldsymbol{P}_{AA'} + {}^{A}_{B}\boldsymbol{R}^{-1}\,{}^{O}_{A}\boldsymbol{R}^{-1}\,{}^{o}_{A'}\boldsymbol{R}\,{}^{A'}\boldsymbol{P}_{A'B'} - {}^{A}_{B}\boldsymbol{R}^{-1}\,{}^{A}\boldsymbol{P}_{AB} \end{aligned} \tag{10} $$

In fact, symbols ${}^{A}_{B}\boldsymbol{R}$, ${}^{A'}_{B'}\boldsymbol{R}$, ${}^{A'}\boldsymbol{P}_{A'B'}$, ${}^{A}\boldsymbol{P}_{AB}$ obtained by parameters of designing, are the transformation and translation matrices between $\boldsymbol{A}$ coordinate system and $\boldsymbol{B}$ coordinate system. They have such relationship

$$ \begin{aligned} {}^{A}_{B}\boldsymbol{R} &= {}^{A'}_{B'}\boldsymbol{R} \\ &= \begin{pmatrix} \cos(\alpha)\cos(\beta) & \cos(\alpha)\sin(\beta)\sin(\gamma) - \cos(\gamma)\sin(\alpha) & \sin(\alpha)\sin(\gamma) + \cos(\alpha)\cos(\gamma)\sin(\beta) \\ \cos(\beta)\sin(\alpha) & \cos(\alpha)\cos(\gamma) + \sin(\alpha)\sin(\beta)\sin(\gamma) & \cos(\gamma)\sin(\alpha)\sin(\beta) - \cos(\alpha)\sin(\gamma) \\ -\sin(\beta) & \cos(\beta)\sin(\gamma) & \cos(\beta)\cos(\gamma) \end{pmatrix} \end{aligned} \tag{11} $$

where, α, β, λ are Euler angles rotating about z axis, y axis, and x axis in sequence from $\boldsymbol{A}$ (or $\boldsymbol{A'}$) coordinate system to $\boldsymbol{B}$ (or $\boldsymbol{B'}$) coordinate system.

Symbols ${}^{A'}\boldsymbol{P}_{A'B'}$, ${}^{A}\boldsymbol{P}_{AB}$ are also the designing parameters of fixture mounted onto the mobile platform, representing the $\boldsymbol{AB}$ vector (or $\boldsymbol{A'B'}$ vector) in the $\boldsymbol{A}$ (or $\boldsymbol{A'}$) coordinate system. They have such relationship

$$ {}^{A}\boldsymbol{P}_{AB} = {}^{A'}\boldsymbol{P}_{A'B'} = [n_1; n_2; n_3] \tag{12} $$

where, n_1, n_2, n_3 are parameters in design.

Symbols ${}^{O}_{A}\boldsymbol{R}$, ${}^{O}_{A'}\boldsymbol{R}$, ${}^{O}\boldsymbol{P}_{AA'}$ are transformation matrices or vector, decided through the process of measurement with Laser Tracker. In Fig. 4 and 5, three points, obtained in the fixture with black target holder and target ball, define a plane and make up the $\boldsymbol{A}$ or $\boldsymbol{A'}$ coordinate system. ${}^{O}\boldsymbol{P}_{AA'}$ means the vector from origin of A coordinate system to origin of $\boldsymbol{A'}$ coordinate system with respect to the $\boldsymbol{O}$ coordinate system.

It should be noted that, angles for rotation from $\boldsymbol{B}$ coordinate system to $\boldsymbol{B'}$ coordinate system are confined by (-20 degree, 20 degree) due to the geometric constraint of the body. Therefore, the solution of Euler angles in transformation matrix ${}^{B}_{B'}\boldsymbol{R}$ will be only one, not multiple solutions.

III. Error Model

As mentioned before, there are two ways computing error model: numerical method and analytical method. Due to the fact that error model through numerical method can be obtained by simple approach without complicated equation derivation, the numerical method is used to obtain error model in this article.

A. Error Model for Kinematic Parameters

For numerical method, with the explanation in section II, the procedure for constructing error model can be concluded as follows: (i) decide the translation and orientation $\boldsymbol{B}$ for mobile platform in advance; (ii) calculate the displacement for prismatic joint with kinematic parameters in theory, using inverse kinematic solution; (iii) give a unit error to $\boldsymbol{i}$ th kinematic parameter and compute the translation and orientation $\boldsymbol{B'}$ for mobile platform with the displacement of prismatic joint obtained in (ii) by forward kinematic solution, using kinematic parameters with error; (iv) compute the difference $\Delta\boldsymbol{B}$ between the translation and orientation in (iii) and that in (i), and the $\boldsymbol{i}$ th column of Jacobi matrix in equation (1) is just the difference; (v) repeat the same procedure from (iii) to (iv) with different kinematic parameter and put the difference into Jacobi matrix; (vi)repeat the procedure from (i) to (v) with different translation and orientation for mobile platform in Jacobi matrix. Fig. 6 depicts the procedure concisely.

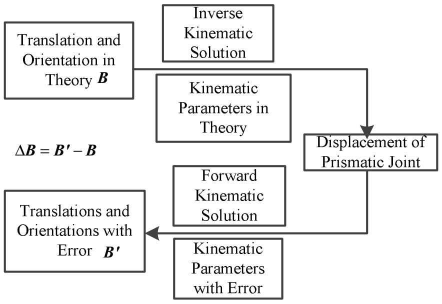

Fig. 6 Construction of error model for parameters in manipulator

In the procedure (i), selection of the translation and orientation for mobile platform is an essential and technical task. Firstly, it should be avoided that the translations and orientations are so linearly correlated that Jacobi matrix in equation (1) tends to singularity. Besides, the translations and orientations will be selected properly to represent the whole work space. Based on former experiences, translations of the mobile platform could be moved with shape of British "Union Jack" from the origin to get several points for measurement. For orientations, the mobile platform could be rotated about the origin with the shape of "Cone" to get several measurements.

In (iii), the translation and orientation for mobile platform is obtained through forward kinematic solution. Usually the forward kinematic solution for parallel manipulator can be computed by numerical method such as Newton-Raphson algorithm. To improve the speed for Newton-Raphson algorithm, such process can be taken: BP neural network could be used firstly to obtain the non-exact forward kinematic solution, namely approximate value; then exact solution would be obtained with Newton-Raphson algorithm. These steps will greatly reduce the cycle number for of Newton-Raphson algorithm and cut down entire time for forward kinematic solution.

B. Error Model for Fixture

The fixture in Fig. 4, mounted onto the mobile platform, has the function of installing the target ball of Laser Tracker. Usually, the fixture is produced and assembled with high accuracy. The black target holder and fixture stick together and the relative position between target holder and fixture will be measured with coordinate measuring machine again to obtain relative position precisely in order to reduce the error as much as possible.

However, it is possible that error exists when fixture is mounted onto the platform during assembly, namely the assembly error. Usually, such error cannot be measured precisely with equipment. Therefore, it is necessary to construct error model considering the assembly error for fixture.

The process to construct error model of fixture involves ${}^{A}_{B}\boldsymbol{R}, {}^{A'}_{B'}\boldsymbol{R}, {}^{A'}\boldsymbol{P}_{A'B'}, {}^{A}\boldsymbol{P}_{AB}$. In other words, parameters for the construction of error model of fixture are α, β, λ in equation (11) and n_1, n_2, n_3 in equation (12).

1) Error Model in Orientation

Before deriving the error model of fixture, it is necessary to understand the meaning of the value in reality and the value in theory. In equation (2), it can be rewritten as:

$$ {}^{B}_{B'}\boldsymbol{R}' = {}^{A}_{B}\boldsymbol{R}^{-1}\, {}^{A}_{A'}\boldsymbol{R}'\, {}^{A'}_{B'}\boldsymbol{R} \tag{13} $$

In equation (13), ${}^{B}_{B'}\boldsymbol{R}'$ and ${}^{A}_{A'}\boldsymbol{R}'$ are transformation matrices considering error of fixture in reality.

$$ {}^{A}_{A'}\boldsymbol{R}' = {}^{A}_{B}\boldsymbol{R}'\, {}^{B}_{B'}\boldsymbol{R}\, {}^{B'}_{A'}\boldsymbol{R}' \tag{14} $$

Transformation matrix ${}^{A}_{A'}\boldsymbol{R}'$ can be derived by equation (14). ${}^{A}_{A'}\boldsymbol{R}'$, ${}^{A}_{B}\boldsymbol{R}'$ and ${}^{B'}_{A'}\boldsymbol{R}'$ are transformation matrices with error, while ${}^{B}_{B'}\boldsymbol{R}$ is the same as parameters in theory.

Let's discuss how errors propagate for the assembly error of fixture mounted onto the mobile platform. Firstly, orientation $\boldsymbol{B}$ is given in advance in theory by ${}^{B}_{B'}\boldsymbol{R}$ in equation (14). In equation (13), during the operation to perform ${}^{B}_{B'}\boldsymbol{R}'$, ${}^{A}_{A'}\boldsymbol{R}'$ can be obtained through measurement with Laser Tracker, while ${}^{A}_{B}\boldsymbol{R}^{-1}$ and ${}^{A'}_{B'}\boldsymbol{R}$ can be obtained by theory in design due to the fact that assembly errors with fixture are unknown in advance. Therefore, errors in ${}^{B}_{B'}\boldsymbol{R}'$ could be only introduced by ${}^{A}_{A'}\boldsymbol{R}'$ when performing the operation of equation (5). In fact, ${}^{A}_{A'}\boldsymbol{R}'$ is obtained through the measurement of movement for mobile platform. In equation (14), ${}^{B}_{B'}\boldsymbol{R}$ is the decided orientation in advance and no error exist in ${}^{B}_{B'}\boldsymbol{R}$. However, as errors with fixture in ${}^{A}_{B}\boldsymbol{R}'$ and ${}^{B'}_{A'}\boldsymbol{R}'$ exist in reality, ${}^{A}_{A'}\boldsymbol{R}'$ in equation (14) involves assembly error produced by fixture mounted onto mobile platform. Therefore, errors in ${}^{B}_{B'}\boldsymbol{R}'$ are related to errors in ${}^{A}_{B}\boldsymbol{R}'$ and ${}^{B'}_{A'}\boldsymbol{R}'$ and can be rewritten as follows:

$$ {}^{B}_{B'}\boldsymbol{R}' = {}^{A}_{B}\boldsymbol{R}^{-1}\, {}^{A}_{B}\boldsymbol{R}'\, {}^{B}_{B'}\boldsymbol{R}\, {}^{B'}_{A'}\boldsymbol{R}'\, {}^{A'}_{B'}\boldsymbol{R} \tag{15} $$

2) Error Model in Translation

The following is the discussion of assembly error of fixture for translation of mobile platform.

$$ {}^{B}\boldsymbol{P}'_{BB'} = {}^{B}\boldsymbol{P}'_{AA'} - {}^{B}\boldsymbol{P}_{AB} + {}^{B}\boldsymbol{R}_{B'}\, {}^{B'}\boldsymbol{P}_{A'B'} \tag{16} $$

${}^{B}\boldsymbol{P}'_{BB'}$ and ${}^{B}\boldsymbol{P}'_{AA'}$ are translation vectors with error in reality, while ${}^{B}\boldsymbol{P}_{AB}$ and ${}^{B}\boldsymbol{R}_{B'}\, {}^{B'}\boldsymbol{P}_{A'B'}$ are translation vectors in theory, the same as those in design.

$$ {}^{B}\boldsymbol{P}'_{AA'} = {}^{B}\boldsymbol{P}'_{AB} + {}^{B}\boldsymbol{P}_{BB'} + {}^{B}\boldsymbol{P}'_{B'A'} \tag{17} $$

${}^{B}\boldsymbol{P}'_{AB}$ and ${}^{B}\boldsymbol{P}'_{B'A'}$ are translation vectors with error in reality, while ${}^{B}\boldsymbol{P}_{BB'}$ is translation vector in theory, the position of the origin of $\boldsymbol{B}'$ coordinate system relative to $\boldsymbol{B}$ coordinate system given in advance.

Let's discuss the propagation of assembly errors of fixture for the translation of mobile platform. The propagation of assembly errors for translation is similar with that for transformation. Firstly, translation is given in advance in theory by ${}^{B}\boldsymbol{P}_{BB'}$ in equation (17). As errors with fixture in ${}^{B}\boldsymbol{P}'_{AB}$ and ${}^{B}\boldsymbol{P}'_{B'A'}$ exist in reality, ${}^{B}\boldsymbol{P}'_{AA'}$ in equation (17) also involves error produced by fixture mounted onto mobile platform. During the operation of performing ${}^{B}\boldsymbol{P}'_{BB'}$ in equation (16), ${}^{B}\boldsymbol{P}'_{AA'}$ can be obtained through measurement with Laser Tracker, and errors in ${}^{B}\boldsymbol{P}'_{AA'}$ are from ${}^{B}\boldsymbol{P'}_{AB}$ and ${}^{B}\boldsymbol{P'}_{B'A'}$ in reality. ${}^{B}\boldsymbol{P}_{AB}$ and ${}^{B}\boldsymbol{R}_{B'}$ ${}^{B'}\boldsymbol{P}_{A'B'}$ can be obtained by theory in design, as errors with fixture are unknown in advance. Therefore, errors in ${}^{B}\boldsymbol{P'}_{BB'}$ involve ${}^{B}\boldsymbol{P'}_{AB}$ and ${}^{B}\boldsymbol{P'}_{B'A'}$, which can be rewritten as follows

$$ {}^{B}\boldsymbol{P'}_{BB'} = {}^{B}\boldsymbol{P'}_{AB} + {}^{B}\boldsymbol{P}_{BB'} + {}^{B}\boldsymbol{P'}_{B'A'} - {}^{B}\boldsymbol{P}_{AB} + {}^{B}_{B'}\boldsymbol{R}\,{}^{B'}\boldsymbol{P}_{A'B'} \quad (18)$$

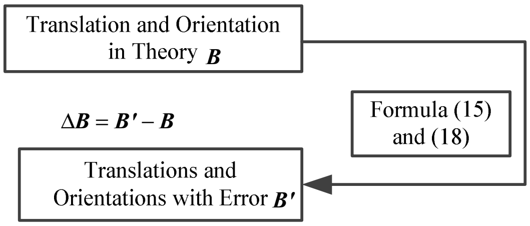

Fig.7 Construction of error model for assembly errors

3) Procedure for constructing error model

Without considering the kinematic parameters for Jacobi matrix in equation (1), the procedure for constructing error model of fixture can be concluded as follows: (i) give the specific translation ${}^{B}\boldsymbol{P}_{BB'}$ and orientation ${}^{B}_{B'}\boldsymbol{R}$ for mobile platform in advance; (ii) give a unit error to $\boldsymbol{i}$ th of parameters $\alpha, \beta, \lambda, n_1, n_2, n_3$, obtaining ${}^{A}_{B}\boldsymbol{R'}$, ${}^{B'}_{A'}\boldsymbol{R'}$, ${}^{B}\boldsymbol{P'}_{AB}$ and ${}^{B}\boldsymbol{P'}_{B'A'}$. Performing the operation of equation (15) and (18) to get ${}^{B}_{B'}\boldsymbol{R'}$ and ${}^{B}\boldsymbol{P'}_{BB'}$; (iii) compute the difference between ${}^{B}\boldsymbol{P'}_{BB'}$ (${}^{B}_{B'}\boldsymbol{R'}$) and ${}^{B}\boldsymbol{P}_{BB'}$ (${}^{B}_{B'}\boldsymbol{R}$), and the $\boldsymbol{i}$ th column of Jacobian matrix in equation (1) for error model of fixture, is just the difference; (iv) repeat the same procedure from (ii) to (iii) with different parameter among $\alpha, \beta, \lambda, n_1, n_2, n_3$ in sequence; (v)give another specific translation ${}^{B}\boldsymbol{P}_{BB'}$ and orientation ${}^{B}_{B'}\boldsymbol{R}$, and repeat process from (i) to (iv). Procedures can be concluded in Fig. 7.

IV. Parameter Identification

A. Particle Swarm Algorithm

The operation to get $\Delta\boldsymbol{X}$ in formula (1) is so called parameter identification. During the process of parameter identification, the particle swarm algorithm is adopted. The particle swarm algorithm is inspired by the group's ability to locate a desirable position. For particle swarm algorithm, a swarm is made up of a set of particles, which delegate potential solutions of a problem for optimization. Considering the $\boldsymbol{i}$ th particle of the swarm, the position and velocity of the particle at iteration t can be depicted as equation (19) and (20). Position and velocity of particle at iteration *t+1* can be performed by the operations (21).

$$\boldsymbol{X}_i(t) = (x_{i,1}(t), x_{i,2}(t), \ldots\ldots x_{i,n}(t)) \quad (19)$$

$$\boldsymbol{V}_i(t) = (v_{i,1}(t), v_{i,2}(t), \ldots\ldots v_{i,n}(t)) \quad (20)$$

$$\begin{cases} v_{i,j}(t+1) = w \times v_{i,j}(t) + r_1 c_1 \times (Pb_{i,j}(t) - x_{i,j}(t)) \\ \qquad + r_2 c_2 \times (Gb_{i,j}(t) - x_{i,j}(t)) \\ x_{i,j}(t+1) = x_{i,j}(t) + v_{i,j}(t+1) \end{cases} \quad (21)$$

$Pb_i(t) = (Pb_{i,1}(t), Pb_{i,2}(t), \ldots\ldots Pb_{i,n}(t))$ is the personal best position, which depicts the best position of the $\boldsymbol{i}$ th particle itself so far. $Gb_i(t) = (Gb_{i,1}(t), Gb_{i,2}(t), \ldots\ldots Gb_{i,n}(t))$ is the global best position, which represents the global best position among neighbors of this particle so far. Acceleration coefficients c_1 and c_2 are acceleration coefficients, which are nonnegative constants affecting the value of $Gb(t)$ and $Pb(t)$ during the exploration process. Avoiding situations of non-convergence, it is suggested $c_1 = c_2 = 2.0$. w is the inertia weight affecting particle's exploration in the search space. It should be noted that a large value of w is beneficial for global search while a small value of w facilitates a local search. r_1 and r_2 are two random numbers within [0,1]. Usually position $x_{i,j}(t)$ and velocity $v_{i,j}(t)$ can be confined within a proper range for the speed of convergence.

The operation of parameter identification involves multi-objective optimization process. The object of multi-objective optimization is to find the Pareto optimal sets [8]. There is another constraint transferring multiple objective functions into single objective function. In this article, the extra constraint is to minimize the function (22)

$$\min \left\| \Delta\boldsymbol{Y} - \boldsymbol{J}\Delta\boldsymbol{X} \right\| \quad (22)$$

Fig.8 shows the entire flowchart of calibration for parallel manipulator which can be used for experiments in practice.

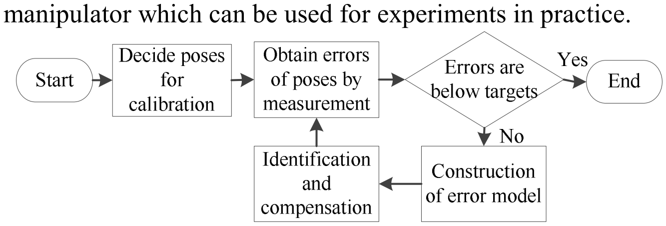

Fig.8 Flowchart of calibration method

V. Experiment

The calibration system in Fig. 9 consists of the Laser Tracker, pc for Laser Tracker, parallel manipulator, target ball, cabinet for controller of motor and pc for controller. Fig. 10 and Fig. 11 are pictures depicting results after calibration. 60 translations and orientations for mobile platform are selected for calibration, and the former 24 groups (called Former 24 Groups) are translations and later 36 groups (called Later 36 Groups) are orientations.

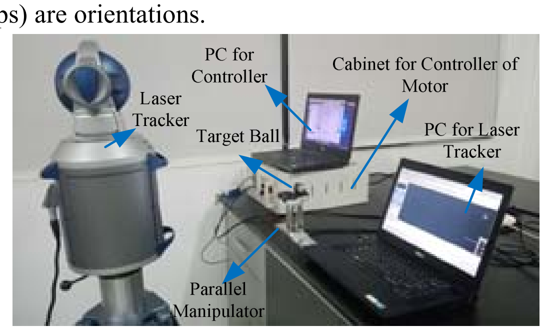

Fig.9 The scene of calibration experiment

For Former 24 Groups, before calibration, the error in translation of mobile platform in Fig.10, is about 1mm while that after calibration is about 0.5mm, dropped by 50%; the error in orientation of mobile platform, in Fig. 11, is about 0.6 while that is 0.2 after calibration, dropped by 66%. For Later

36 Groups, the error in translation of mobile platform, in Fig. 10, is about 0.6mm while that is 0.3mm after calibration, dropped by 50%; in Fig. 11, the error in orientation of mobile platform, is about 1.6 before calibration while that is 0.8 after calibration, dropped by 50%.

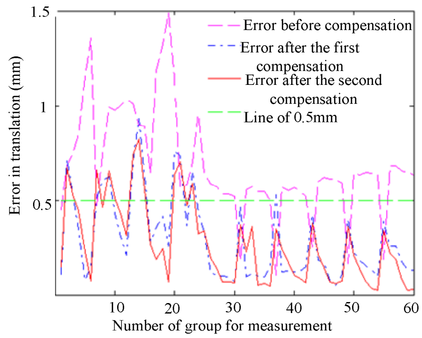

Fig. 10 Error in translation of calibration experiment

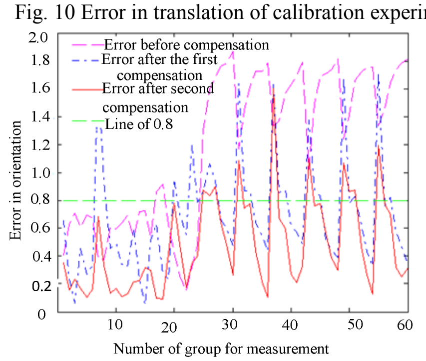

Fig. 11 Error in orientation of calibration experiment

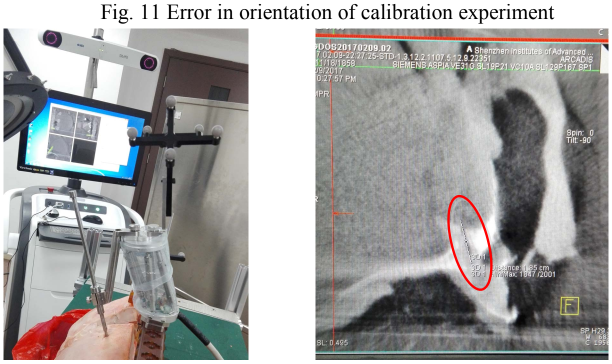

(a) The scene of experiment (b) The result from C-arm

Fig. 12 The experiment with spine of pig

Fig. 12 is the picture depicting the result of pedicle screw placement experiment with spine of pig, using parallel manipulator after calibration. The screw path is just in the direction of vertebra pedicle. It can be concluded that, the parallel manipulator possesses high precision after calibration.

VI. Conclusion

In this paper, surgery robot for pedicle screw placement based on parallel manipulator is introduced. For high precision of mobile platform, practical calibration method is explored particularly. A novel measurement scheme for calibration is proposed with Laser Tracker. Based on the measurement scheme, how to compute the translation and orientation of mobile platform is explored. During the construction of error model, the propagation of error of kinematic parameters, as well as assembly error of fixture, is explored before the construction of error model. Besides, the process to build Jacobi matrix is discussed specifically for the error of kinematic parameters and assembly error of fixture mounted onto mobile platform. Particle swarm algorithm is used for identifying parameters in the process of parameters identification. In the end, experiment of calibration is conducted to verify the effectiveness of the algorithm of calibration. Experiment of pedicle screw placement with spine of pig is carried out to support the precision of the parallel manipulator after calibration.

Acknowledgment

This work is supported by the National High-tech R&D Program of China (No. 2015AA043201) and the National Natural Science Foundation of China (No. U1613224), in part by Shenzhen Fundamental Research Funds (No. JCYJ20150529143500954, JCYJ20160229202315086 and JCYJ20170307170252420).

References

[1] J. J. Santos-Munn´e, M. A. Peshkin, S. Mirkovic, S. D. Stulberg and T. C. Kienzle, "A Stereotactic/Robotic System for Pedicle Screw Placement," *Proceedings of the 3rd Medicine Meets Virtual Reality Conference*, San Diego, USA, pp. 326-333, 1995.

[2] H. Jin, Y. Hu, W. Tian, P. Zhang, Z. Song, J. Zhang and B. Li, "Kinematic and cooperative control of a robotic spinal surgery system," *Robotica*, vol. 34, no. 01, pp. 226-242, 2016.

[3] D. Togawa, M. M. Kayanja, M. K. Reinhardt, M. Shoham, A. Balter, A. Friedlander, N. Knoller, E.C. Benzel and I. H.Lieberman, "Bone-mounted miniature robotic guidance for pedicle screw and translaminar facet screw placement: Part II—Evaluation of system accuracy," *Neurosurgery*, vol. 60, no. 01, pp. 129-139, 2006.

[4] S. Bai and M. Y. Teo, "Kinematic calibration and pose measurement of a medical parallel manipulator by optical position sensors," *Journal of Robotic Systems*, vol. 20, no. 04, pp. 201-209, 2003.

[5] G. Du, H. Shao, Y. Chen, P. Zhang and X. Liu, "An online method for serial robot self-calibration with CMAC and UKF," *Robotics and Computer-Integrated Manufacturing*, vol. 42, pp. 39-48, 2016.

[6] X. Zhang, W. Yang, X. Cheng and W. Zhu, "A Practical Calibration Method for Spray Painting Robot in Factory," *ICIRA*, Berlin, Heidelberg, pp.164-173, 2012.

[7] W. Liu, D. Tang and Z. Wang, "Cocktail Method for Stewart Platform Calibration," *Chinese Journal of Mechanical Engineering*, vol. 40, no. 12, pp. 48-52, 2004.

[8] Y. Zhang, D. Gong and Z. Ding, "A Bare-Bones Multi-objective Particle Swarm Optimization Algorithm for Environmental/Economic Dispatch," *Information Science*, vol. 192, pp. 213-227, 2012.